

New chalcogen derivatives of silicon possessing adamantane and noradamantane structures

U. Herzog^{a,*}, G. Rheinwald^b

^a Institut für Anorganische Chemie der TU Bergakademie Freiberg, Leipziger Str. 29, D-09596 Freiberg, Germany

^b Institut für Chemie der TU Chemnitz, Straße der Nationen 62, D-09111 Chemnitz, Germany

Received 8 September 2000; received in revised form 14 December 2000; accepted 18 December 2000

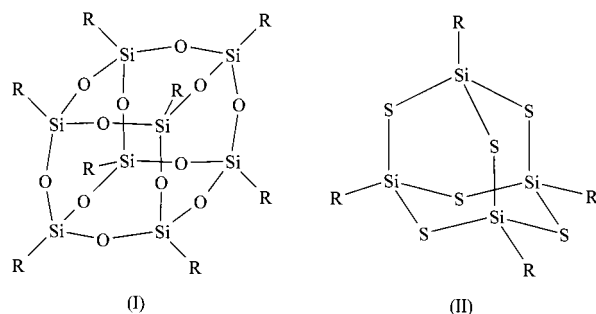
Abstract

The reaction of $\text{Si}_2\text{Cl}_4\text{Me}_2$ (**1**) with Li_2Se in THF yields exclusively the noradamantane $(\text{MeSi})_4\text{Se}_5$ (**4**). The sulfur analogue $(\text{MeSi})_4\text{S}_5$ (**3**) could be obtained from **1**, MeSiCl_3 , H_2S and NEt_3 . Reactions of the disilylmethane $\text{CH}_2(\text{SiMeCl}_2)_2$ (**5c**) with either $\text{H}_2\text{S}/\text{NEt}_3$ or Li_2E ($\text{E} = \text{Se}, \text{Te}$) produced the new adamantanes $(\text{MeSi})_4(\text{CH}_2)_2\text{E}_4$ ($\text{E} = \text{S}$ (**6**), Se (**7**) and Te (**8**)). Similar reactions of mixtures of **1** and **5c** resulted in the formation of the noradamantanes $(\text{MeSi})_4(\text{CH}_2)\text{E}_4$ ($\text{E} = \text{S}$ (**9**), Se (**10**)). All compounds were characterized by multinuclear NMR spectroscopy. The crystal structures of **3**, **6**, **7**, **8**· CDCl_3 and **9** are reported. © 2001 Elsevier Science B.V. All rights reserved.

Keywords: Silthianes; Sulfur; Selenium; Tellurium; Noradamantane

1. Introduction

While polyhedral oligosilsesquioxanes (POSS), which have received much attention in recent years [1–4], form cube-octameric $\text{R}_8\text{Si}_8\text{O}_{12}$ (I) or even larger cages, silsesquithianes (and -selenanes) usually adopt adamantane like structures (II) due to the much smaller bond angle SiSSi (Scheme 1).



Scheme 1. Structures of $\text{R}_8\text{Si}_8\text{O}_{12}$ (I) and $\text{R}_4\text{Si}_4\text{S}_6$ (II).

* Corresponding author. Tel.: +49-3731-394343; fax: +49-3731-394058.

E-mail address: herzog@merkur.hrz.tu-freiberg.de (U. Herzog).

A variety of silsesquithianes and -selenanes [5–7] as well as the related germanium [8–10] and tin [11–14] compounds have been prepared by different methods, but in most cases reactions of RMX_3 ($\text{M} = \text{Si}, \text{Ge}, \text{Sn}$; $\text{X} = \text{Cl}, \text{Br}$) with H_2E ($\text{E} = \text{S}, \text{Se}$) in the presence of a base such as NEt_3 or pyridine were applied.

Table 1 summarizes some characteristic bond lengths and angles of this class of compounds. It can be seen, that in all these molecules the angles at the chalcogen atom are smaller than the ideal tetrahedral angle of 109.5° while the angles EME are slightly expanded. The angles deviate more from the tetrahedral angle if R is an electron withdrawing substituent like C_6F_5 or CF_3 . In the cases of sterically demanding substituents R the reactions with Li_2S or Li_2Se yielded double-decker like structures $[(\text{RME})_2\text{E}]_2$ ($\text{R} = 1,1,2\text{-trimethylpropyl}$; $\text{M} = \text{Si}, \text{Ge}$; $\text{E} = \text{S}, \text{Se}$ [15]; $\text{R} = \textit{t}\text{-butyl}$; $\text{M} = \text{Si}, \text{E} = \text{S}$ [16]; $\text{R} = \text{CpFe}(\text{CO})_2$; $\text{M} = \text{Si}, \text{E} = \text{Se}$ [17]). The sulfur compounds tend to isomerize to the more stable adamantane derivatives on heating to 200°C [15,16]. Ando et al. attempted the synthesis of silicon and germanium chalcogenanes possessing bisnoradamantane structures by reacting $\textit{t}\text{-BuMCl}_2\text{-MCl}_2\textit{t}\text{-Bu}$ ($\text{M} = \text{Si}, \text{Ge}$) with Li_2E ($\text{E} = \text{S}, \text{Se}$). While the expected bisnoradamantane (III) could be isolated for $\text{M} = \text{Ge}$ and $\text{E} = \text{S}$, the reactions for $\text{M} = \text{Si}$ and $\text{E} = \text{S}$ or Se resulted in cleavage of one

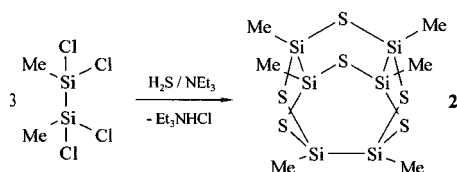
Table 1

Important bond parameters of silsesquichalcogenides and related germanium and tin compounds (RM)₄E₆ possessing an adamantane structure

R	M	E	<i>d</i> _{ME} (Å)	∠ EME (°)	∠ MEM (°)	Ref.
H	Si	S	2.133, 2.137	112.0, 113.0	102.2, 103.0	[6]
Me	Si	S	2.129	111.8	104.5	[5]
Me	Ge	S	2.20–2.22	110.8–112.5	104.2–105.0	[8]
CF ₃	Ge	S	2.210	113.8	99.9	[10]
CF ₃	Ge	Se	2.344	114.8	97.3	[10]
Me	Sn	S	2.38–2.40	109.6–113.1	105.4–106.1	[11,12]
C ₆ F ₅	Sn	S	2.38–2.41	110.0–114.8	102.7–104.3	[13]
Me	Sn	Se	2.51–2.54	110.1–115.2	102.1–103.7	[14]

SiSi bond and formation of the noradamantanes (IV) in low yields (20 and 14%) [18] (Scheme 2).

In contrast to these reactions with lithium chalcogenides, the reaction of MeCl₂Si–SiCl₂Me (**1**) with H₂S and NEt₃ yielded a cage compound **2** containing three disilane units without cleavage of SiSi bonds [19]:

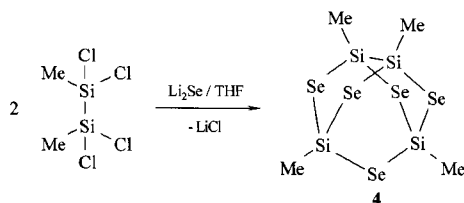


DFT calculations have shown, that in this case the observed tetracyclic cage compound is by 59 kJ mol⁻¹ more stable than 1.5 molecules of the corresponding bisnoradamantane [19].

2. Results and discussion

2.1. Noradamantanes (MeSi)₄E₅ (E = S, Se)

In contrast to the formation of a cage compound **2** in the reaction of **1** with H₂S and NEt₃ the reaction of **1** with Li₂Se (prepared from Se and Li[BET₃H]) yielded exclusively the noradamantane **4**.



As expected, two ⁷⁷Se-NMR signals could be observed in a 4:1 ratio. Furthermore the ¹J_{SiSe} and ²J_{SiSe} satellites at Si^A and two different ¹J_{SiSe} satellites in a 1:2 ratio at Si^B in the ²⁹Si-NMR spectrum prove the assignment as a noradamantane.

The reaction of **1** with Li₂Te under the same conditions yielded no isolable products.

The analogous sulfur compound **3** could be prepared by reacting a mixture of one and two equivalents of MeSiCl₃ with H₂S and NEt₃.

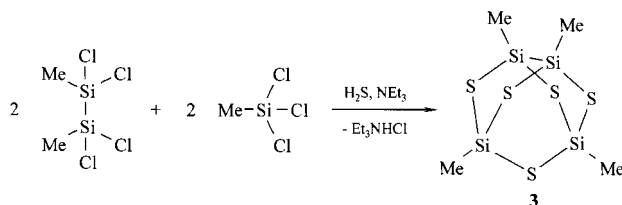
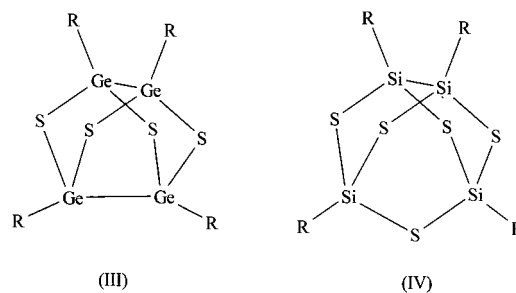


Fig. 1 shows the molecular structure of one of the two crystallographically independent molecules of **3** in the asymmetric unit, characteristic bond distances and angles are given in Table 2.



Scheme 2. Structures of bis-noradamantanes (III) and noradamantanes (IV).

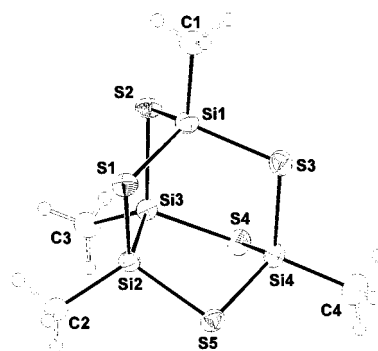


Fig. 1. Molecular structure of one of the two independent molecules of **3**.

Table 2
Important bond lengths (Å) and bond angles (°) of one of the two independent molecules of **3**

Bond lengths			
S(1)–Si(1)	2.1453(16)	S(5)–Si(4)	2.1540(16)
S(1)–Si(2)	2.1505(13)	S(5)–Si(2)	2.1606(14)
S(2)–Si(1)	2.1498(12)	Si(1)–C(1)	1.855(4)
S(2)–Si(3)	2.1580(14)	Si(2)–C(2)	1.851(5)
S(3)–Si(1)	2.1524(15)	Si(3)–C(3)	1.857(4)
S(3)–Si(4)	2.1628(14)	Si(4)–C(4)	1.845(5)
S(4)–Si(3)	2.1550(14)	Si(2)–Si(3)	2.3729(14)
S(4)–Si(4)	2.1483(13)		
Bond angles			
Si(1)–S(1)–Si(2)	94.12(5)	S(1)–Si(2)–Si(3)	105.88(6)
Si(1)–S(2)–Si(3)	94.41(5)	S(5)–Si(2)–Si(3)	105.18(6)
Si(1)–S(3)–Si(4)	106.65(6)	S(4)–Si(3)–S(2)	110.15(6)
Si(4)–S(4)–Si(3)	94.74(5)	S(4)–Si(3)–Si(2)	104.93(5)
Si(4)–S(5)–Si(2)	94.74(5)	S(2)–Si(3)–Si(2)	104.21(5)
S(1)–Si(1)–S(2)	108.75(6)	S(4)–Si(4)–S(5)	108.61(6)
S(1)–Si(1)–S(3)	110.46(6)	S(4)–Si(4)–S(3)	110.53(6)
S(2)–Si(1)–S(3)	112.01(6)	S(5)–Si(4)–S(3)	111.57(6)
S(1)–Si(2)–S(5)	109.51(6)		

The silicon sulfur as well as the silicon carbon bond lengths are in the usual range while the Si–Si bond is slightly longer than in normal disilanes [20] bearing no

bulky substituents. The two five membered rings adopt envelope conformations with angles between the two planes of 59.4 and 59.5°. The bond angle Si(1)–S(3)–Si(4), which is part of six-membered rings only is by more than 10° larger than the other Si–S–Si angles which are also incorporated in five-membered rings. This difference has also been found in other polycyclic silthianes [19].

The sulfur atoms form a tetragonal pyramid with an almost ideal square as base. The S–S distances in the sulfur square lie in the range of 3.49–3.54 Å, which is by 0.2 Å less than twice the van der Waals radius of sulfur (3.7 Å). The S–S distances to the sulfur atom at the top of the pyramid are in the range of 3.53–3.57 Å. The nonbonding silicon–silicon distances between silicon atoms of the disilane unit and one of the other two Si atoms are between 3.14 and 3.17 Å, and the distance Si(1)–Si(4) is 3.461 Å, while twice the van der Waals radius of silicon would be 4 Å.

The NMR data of **3** and **4** are summarized and compared with those of the related adamantane compounds (MeSi)₄E₆ in Table 3.

A comparison of the ²⁹Si-NMR shifts of the silsesquichalcogenanes (MeSi)₄E₆ with the acyclic compounds MeSi(SBu)₃ (δ_{Si}: 29.5 ppm) [21] and Me-

Table 3
NMR data of the silsesquichalcogenides Me₄Si₄E₆ and noradamantanes Me₄Si₄E₅ (E = S, Se) (chemical shifts in ppm, coupling constants in Hz)

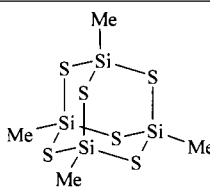
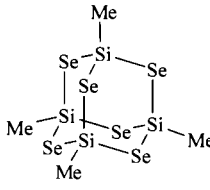
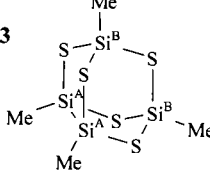
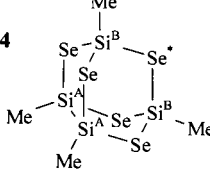
compound	δ _{Si}	δ _{Se}	¹ J _{SiSe}	δ _C	¹ J _{SiC}	δ _H
	17.2	-	-	10.9		1.05
	-0.2	-89	157.5	11.9		1.37 ³ J _{Sett} : 7
3 	A: 23.9 B: 27.7	-	-	A: 1.8 B: 8.8	53.0 65.6	1.05, 1.06 (1:1)
4 	A: 28.9 B: 3.5	Se: -53 Se*: -12	134.1 (Si ^A Se), ² J _{SiSe} : 9.2 147.7 (Si ^B Se) 156.5 (Si ^B Se*)	A: 2.6 B: 10.4		A: 1.22 B: 1.34

Table 4

¹H-, ¹³C- and ²⁹Si-NMR data of disilylmethanes **5a–c**, Cl_iMe_{3–i}Si–CH₂–SiCl_jMe_{3–j} (*i, j* = 1, 2) (chemical shifts in ppm, coupling constants in Hz)

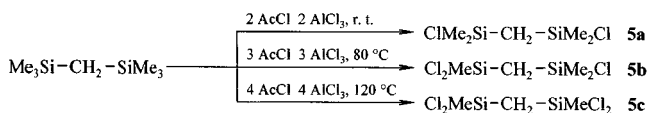
Compound	δ_{Si}	δ_{C}		δ_{H}	
		CH ₃	CH ₂	CH ₃	CH ₂
ClMe ₂ Si–CH ₂ –SiClMe ₂ (5a)	28.5	4.3; ¹ J _{SiC} : 58.3	10.9; ¹ J _{SiC} : 49.1	0.49	0.565
Cl ₂ MeSi ^A –CH ₂ –Si ^B ClMe ₂ (5b)	A: 27.0; B: 28.3	A: 7.85; B: 4.1	14.3	A: 0.87; B: 0.56	0.92
Cl ₂ MeSi–CH ₂ –SiCl ₂ Me (5c)	25.9	7.5; ¹ J _{SiC} : 71.1	17.5; ¹ J _{SiC} : 59.9	0.93	1.28

Si(SeBu)₃ (δ_{Si} : 13.5 ppm) [22] having the same first coordination sphere at silicon reveal high field shifts of 12.3 and 13.7 ppm, respectively, in accordance with the fact that the silicon atoms in the adamantanes are part of six-membered rings, and the formation of this ring size is usually accompanied by a ²⁹Si-NMR high field shift [19,23]. In the noradamantanes **3** and **4** the disilane units are part of five-membered rings, and as expected, the ²⁹Si-NMR shifts are shifted to lower field in comparison with the acyclic disilanes 1,2-Me₂Si₂(SBu)₄ (δ_{Si} : 9.1 ppm) [21] and 1,2-Me₂Si₂(SeBu)₄ (δ_{Si} : –1.1 ppm) [22] by 14.8 ppm in **3** and 30.0 ppm in **4**. On the other hand the two monosilyl units in **3** and **4** are part of both, five- and six-membered rings, which in its sum results in a high field shift of 1.8 ppm for the sulfur compound **3** versus MeSi(SBu)₃ and 10.0 ppm for the selenium compound **4** versus MeSi(SeBu)₃.

2.2. Silchalcogenanes (MeSi)₄(CH₂)₂E₄ (**6–8**)

2.2.1. Preparation of Cl₂MeSiCH₂SiMeCl₂ (**5c**)

Chlorosubstituted disilylmethanes are formed as minor by-products in the direct process, i.e. reaction of silicon with methyl chloride, but can not be separated from this product mixture. The reaction of (Me₃Si)₂CH₂ with acetyl chloride (AcCl) and aluminium chloride [24] gave, depending on the reaction conditions, ClMe₂SiCH₂SiClMe₂ (**5a**), Cl₂MeSiCH₂–SiClMe₂ (**5b**) or Cl₂MeSiCH₂–SiMeCl₂ (**5c**):

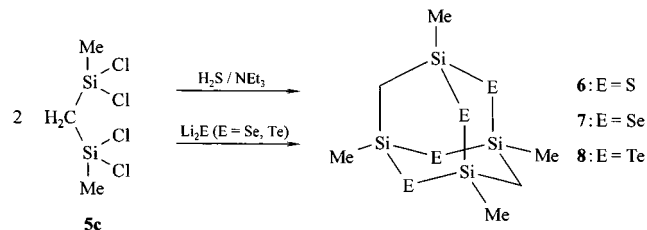


The ²⁹Si-NMR data of all chlorosubstituted disilylmethanes Cl_iMe_{3–i}Si–CH₂–SiCl_jMe_{3–j} have been reported in [25] but our own results differ slightly from literature values. The observed ¹H-, ¹³C- and ²⁹Si-NMR chemical shifts of disilylmethanes are summed up in Table 4.

2.2.2. Formation of (MeSi)₄(CH₂)₂E₄ (E = S (**6**), Se (**7**), Te (**8**))

In a clean reaction treatment of disilylmethane **5c** with H₂S and NEt₃ yielded adamantane **6** containing two methylene units in the cage.

The analogous selenium and tellurium compounds **7** and **8** could be prepared by reaction of **5c** with two equivalents of Li₂Se or Li₂Te, respectively:



The crystal structures of all three products could be determined. To our knowledge **8**·CDCl₃ is the first siltellurane with an adamantane structure, and only a small number of crystal structure analyses of compounds containing a Si–Te bond are known, e.g. C₆H₄(NR)₂Si(Te)₂Si(NR)₂C₆H₄ [26], 'Bu₂Si(Te)₂Si' Bu₂ [27], (Me₃Si)₂Te (no crystal structure analysis), (Me₃Si)₃SiTeH [28] and some derivatives [29–32], Ph₃SiTeH [33], Mes₄Si₂Te [34] or (Cp₂Si)₂Te₃ [35]. This is likely because of the high reactivity of the Si–Te bond. While crystalline silthianes like **6** can be handled in air for some minutes without decomposition, the silselenane **7** slowly turns red under formation of selenium, and siltelluranes like **8** decompose in air immediately into black elemental tellurium and siloxanes. Solutions of these compounds are even more sensitive towards moisture and air.

Figs. 2–4 illustrate the molecular structures of **6**, **7** and **8** showing the adamantane cages which become

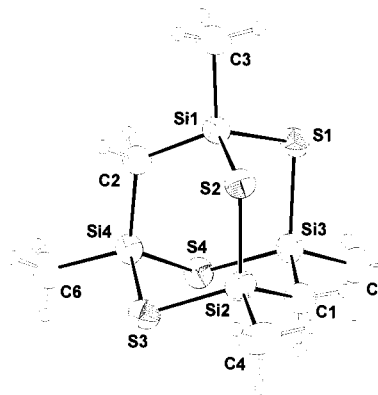
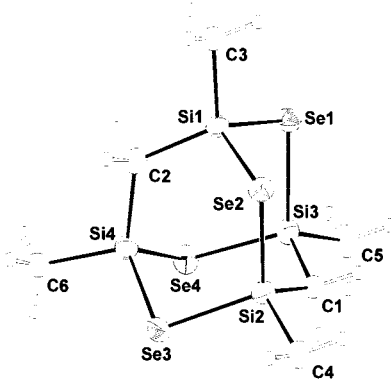
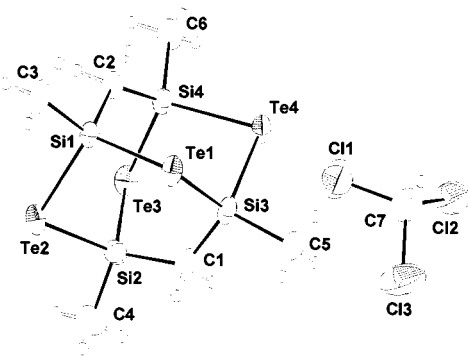


Fig. 2. ORTEP plot of the molecular structure of **6**.

Fig. 3. ORTEP plot of the molecular structure of **7**.Fig. 4. ORTEP plot of the molecular structure of **8**·CDCl₃.

more and more distorted going down the Group 16 elements (S, Se, Te). The characteristic bond parameters of **6–8** are given in Tables 5–7.

The bond lengths Si–C and Si–E (E = S, Se, Te) are all in the expected range. In all three structures the four chalcogen atoms span an almost ideal square with edge lengths of d_{SS} : 3.51–3.53 Å in **6**, d_{SeSe} : 3.73–3.77 Å in **7** and d_{TeTe} : 4.07–4.11 Å in **8**·CDCl₃. But due to the increasing bond lengths Si–S < Si–Se < Si–Te and the fact that the bond angles at E tend to decrease in the series S–Se–Te the octahedron of the four E atoms and the two methylene carbons (C1 and C2) becomes more and more flattened which can be seen by the increasing ratio $d(E(1)–E(3))/d(C(1)–C(2))$ and the decreasing Si–E–Si and increasing Si–C–Si angles, Table 8. In an ideal adamantane cage both ratios, $d(E(1)–E(3))/d(C(1)–C(2))$ and $\angle(\text{SiCSi})/\angle(\text{SiESi})$, should be equal to unity.

The tendency of tellurium to form such small bond angles (Si–Te–Si: 93.6–94.2° in **8**·CDCl₃) may be the reason why no organosilsesquitelluranes have been reported so far and also our own attempts to isolate such a compound failed while the corresponding sulfur and selenium compounds are well known.

In Table 9 the ¹H-, ¹³C-, ²⁹Si-, ⁷⁷Se- and ¹²⁵Te-NMR data of **6–8** are summarized, as well as those of the

Table 5
Important bond lengths (Å) and bond angles (°) of **6**

<i>Bond lengths</i>			
Si(1)–Si(1)	2.1446(12)	Si(1)–C(2)	1.866(3)
Si(1)–Si(3)	2.1479(13)	Si(1)–C(3)	1.860(4)
Si(2)–Si(1)	2.1461(12)	Si(2)–C(1)	1.845(4)
Si(2)–Si(2)	2.1475(13)	Si(2)–C(4)	1.880(4)
Si(3)–Si(2)	2.1323(13)	Si(3)–C(1)	1.850(4)
Si(3)–Si(4)	2.1439(12)	Si(3)–C(5)	1.873(4)
Si(4)–Si(3)	2.1399(13)	Si(4)–C(2)	1.856(3)
Si(4)–Si(4)	2.1408(12)	Si(4)–C(6)	1.853(4)
<i>Bond angles</i>			
Si(1)–Si(1)–Si(3)	101.11(5)	Si(3)–Si(2)–S(2)	110.47(6)
Si(1)–Si(2)–Si(2)	101.20(5)	S(4)–Si(3)–S(1)	110.75(5)
Si(2)–S(3)–Si(4)	101.62(6)	S(4)–Si(4)–S(3)	110.32(5)
Si(3)–S(4)–Si(4)	101.40(5)	Si(2)–C(1)–Si(3)	118.4(2)
Si(1)–Si(1)–S(2)	109.78(5)	Si(4)–C(2)–Si(1)	119.4(2)

Table 6
Important bond lengths (Å) and bond angles (°) of **7**

<i>Bond lengths</i>			
Se(1)–Si(1)	2.278(2)	Si(1)–C(2)	1.870(5)
Se(1)–Si(3)	2.276(2)	Si(1)–C(3)	1.855(5)
Se(2)–Si(1)	2.277(2)	Si(2)–C(1)	1.866(6)
Se(2)–Si(2)	2.278(2)	Si(2)–C(4)	1.859(5)
Se(3)–Si(2)	2.283(2)	Si(3)–C(1)	1.869(6)
Se(3)–Si(4)	2.281(2)	Si(3)–C(5)	1.864(6)
Se(4)–Si(3)	2.285(2)	Si(4)–C(2)	1.863(5)
Se(4)–Si(4)	2.280(2)	Si(4)–C(6)	1.865(6)
<i>Bond angles</i>			
Si(1)–Se(1)–Si(3)	98.41(6)	Se(3)–Si(2)–Se(2)	110.88(7)
Si(1)–Se(2)–Si(2)	98.39(5)	Se(4)–Si(3)–Se(1)	109.64(7)
Si(2)–Se(3)–Si(4)	98.08(6)	Se(4)–Si(4)–Se(3)	109.71(7)
Si(3)–Se(4)–Si(4)	98.26(6)	Si(2)–C(1)–Si(3)	122.4(3)
Se(1)–Si(1)–Se(2)	111.71(7)	Si(4)–C(2)–Si(1)	122.7(3)

Table 7
Important bond lengths (Å) and bond angles (°) of **8**·CDCl₃

<i>Bond lengths</i>			
Te(1)–Si(1)	2.511(2)	Si(2)–C(1)	1.881(8)
Te(1)–Si(3)	2.507(2)	Si(2)–C(4)	1.825(16)
Te(2)–Si(1)	2.491(2)	Si(3)–C(1)	1.847(13)
Te(2)–Si(2)	2.496(2)	Si(3)–C(5)	1.863(7)
Te(3)–Si(2)	2.503(2)	Si(4)–C(2)	1.879(8)
Te(3)–Si(4)	2.501(2)	Si(4)–C(6)	1.861(12)
Te(4)–Si(3)	2.499(2)	C(7)–Cl(1)	1.750(9)
Te(4)–Si(4)	2.497(2)	C(7)–Cl(2)	1.735(12)
Si(1)–C(2)	1.854(10)	C(7)–Cl(3)	1.777(16)
Si(1)–C(3)	1.863(8)		
<i>Bond angles</i>			
Si(1)–Te(1)–Si(3)	93.83(7)	Te(4)–Si(4)–Te(3)	108.86(9)
Si(1)–Te(2)–Si(2)	94.20(9)	Si(2)–C(1)–Si(3)	127.2(6)
Si(2)–Te(3)–Si(4)	93.57(10)	Si(4)–C(2)–Si(1)	128.0(5)
Si(3)–Te(4)–Si(4)	93.86(8)	Cl(1)–C(7)–Cl(2)	111.5(7)
Te(1)–Si(1)–Te(2)	109.77(10)	Cl(1)–C(7)–Cl(3)	109.3(9)
Te(3)–Si(2)–Te(2)	109.41(9)	Cl(2)–C(7)–Cl(3)	109.7(6)
Te(4)–Si(3)–Te(1)	110.60(11)		

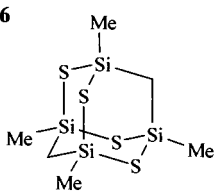
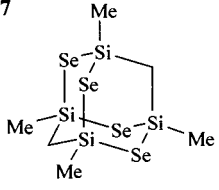
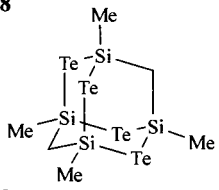
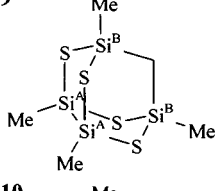
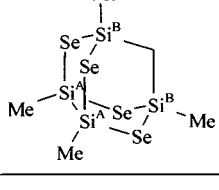
Table 8
Comparison of some geometric parameters of the compounds $\text{Me}_4\text{Si}_4\text{E}_4(\text{CH}_2)_2$, E = S (6), Se (7), Te (8) with an adamantane skeleton

Parameter	6 (E = S)	7 (E = Se)	8 (E = Te)
$d(\text{C}(1)-\text{C}(2))$ (Å)	4.31	4.35	4.43
$d(\text{E}(1)-\text{E}(3))$ and $d(\text{E}(2)-\text{E}(4))$ (Å)	4.97	5.30	5.77, 5.79
$d(\text{E}(1)-\text{E}(3))/d(\text{C}(1)-\text{C}(2))$	1.15	1.22	1.30
Average $\angle(\text{SiCSi})/\angle(\text{SiESi})$	1.17	1.25	1.36

noradamantanes **9** and **10**. In order to estimate the effects of the adamantane cage on the ^{29}Si -NMR shifts one can compare the values of **6–8** with those of the acyclic compounds $\text{Me}_2\text{Si}(\text{EBu})_2$ of 24.8 ppm (E = S)

[21], 18.1 ppm (E = Se) [22] and -24.6 ppm (E = Te) [36] and the monocyclic six-membered ring compounds $(\text{Me}_2\text{SiE})_3$ of 21.1 ppm (E = S), 15.2 ppm (E = Se) and -23.7 ppm (E = Te) [37] having the same first coordination sphere at silicon. It is obvious, that in comparison with the acyclic compounds the formation of a six-membered ring $(\text{Me}_2\text{SiE})_3$ is accompanied by a high field shift of 3–4 ppm for E = S, Se but a small down field shift of 0.9 ppm for E = Te, and in an adamantane structure, where the silicon atom is incorporated into three six-membered rings, a further high field shift of 1.4 ppm (E = S), 5.3 ppm (E = Se) and 16.1 ppm (E = Te) occurs. Compared with the six-membered rings $(\text{Me}_2\text{SiE})_3$ the ^{77}Se - and ^{125}Te -NMR shifts increase from $\delta_{\text{Se}} = -244$ ppm in $(\text{Me}_2\text{SiSe})_3$ by 46 ppm in **7** and from $\delta_{\text{Te}} = -618$ ppm in $(\text{Me}_2\text{SiTe})_3$ by 125 ppm in **8** while the coupling constants $^1J_{\text{SiE}}$ decrease slightly

Table 9
NMR data of the tetrachalcogenadamantanes $\text{Me}_4\text{Si}_4(\text{CH}_2)_2\text{E}_4$ (E = S, Se, Te) and -noradamantanes $\text{Me}_4\text{Si}_4(\text{CH}_2)\text{E}_4$ (E = S, Se) (chemical shifts in ppm, coupling constants in Hz)

compound	δ_{Si}	δ_{E}	$^1J_{\text{SiE}}$	δ_{C}	$^1J_{\text{SiC}}$	δ_{H}
6 	19.7	-	-	Me: 8.4 CH ₂ : 13.1	62.3 51.9	0.74 0.82
7 	9.9	Se: -198	128.3	Me: 9.5, $^2J_{\text{SeC}}$: 16.8 CH ₂ : 12.1	57.3	0.91 0.92
8 	-39.8	Te: -493	329.5	Me: 10.9, $^2J_{\text{TeC}}$: 36.8 CH ₂ : 4.6	50.5 43.3	1.24, $^3J_{\text{TeH}}$: 15 0.87
9 	A: 23.1 B: 28.6	-	-	A: 1.3 B: 6.6 CH ₂ : 15.3	51.9 59.9 51.9	A: 1.00 B: 0.80 CH ₂ : 0.67
10 	A: 22.95 B: 17.8	Se: -124	131.5 $^2J_{\text{SiSe}}$: 8.0	A: 1.9 B: 8.15 CH ₂ : 13.9	46.4 55.4 49.1	A: 1.17 B: 0.97 CH ₂ : 0.95

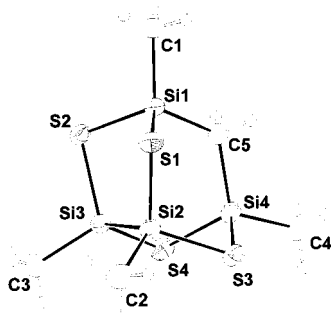


Fig. 5. ORTEP plot of one of the two independent molecules in the crystal structure of **9**.

Table 10

Important bond lengths (Å) and bond angles (°) of the two independent molecules of **9** {S(5)–S(8) and Si(5)–Si(8) are equivalent to S(1)–S(4) and Si(1)–Si(4), C(6)–C(10) to C(1)–C(5)}.

Bond lengths

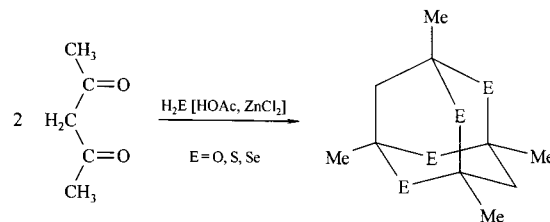
S(1)–Si(1)	2.1533(7)	S(5)–Si(5)	2.1506(7)
S(1)–Si(2)	2.1364(7)	S(5)–Si(6)	2.1446(7)
S(2)–Si(1)	2.1463(7)	S(6)–Si(5)	2.1533(8)
S(2)–Si(3)	2.1387(7)	S(6)–Si(7)	2.1490(7)
S(3)–Si(2)	2.1452(7)	S(7)–Si(6)	2.1449(7)
S(3)–Si(4)	2.1531(8)	S(7)–Si(8)	2.1538(7)
S(4)–Si(3)	2.1493(8)	S(8)–Si(7)	2.1465(7)
S(4)–Si(4)	2.1542(8)	S(8)–Si(8)	2.1468(8)
Si(2)–Si(3)	2.3769(8)	Si(6)–Si(7)	2.3726(8)
Si(1)–C(1)	1.846(2)	Si(5)–C(6)	1.856(2)
Si(2)–C(2)	1.859(2)	Si(6)–C(7)	1.856(2)
Si(3)–C(3)	1.855(2)	Si(7)–C(8)	1.848(2)
Si(4)–C(4)	1.853(2)	Si(8)–C(9)	1.849(2)
Si(1)–C(5)	1.870(2)	Si(5)–C(10)	1.865(2)
Si(4)–C(5)	1.864(2)	Si(8)–C(10)	1.869(2)

Bond angles

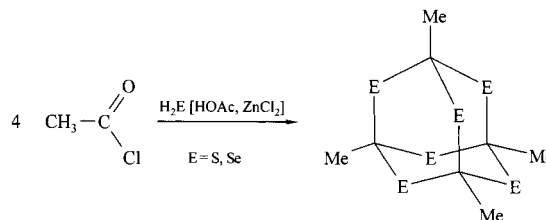
Si(1)–S(1)–Si(2)	92.96(3)	Si(5)–S(5)–Si(6)	93.06(3)
Si(1)–S(2)–Si(3)	93.17(3)	Si(5)–S(6)–Si(7)	92.82(3)
Si(2)–S(3)–Si(4)	92.74(3)	Si(6)–S(7)–Si(8)	92.64(3)
Si(3)–S(4)–Si(4)	92.71(3)	Si(7)–S(8)–Si(8)	92.84(3)
S(1)–Si(1)–S(2)	107.66(3)	S(5)–Si(5)–S(6)	107.78(3)
S(1)–Si(2)–S(3)	109.89(3)	S(5)–Si(6)–S(7)	109.08(3)
S(2)–Si(3)–S(4)	110.16(3)	S(6)–Si(7)–S(8)	110.03(3)
S(3)–Si(4)–S(4)	107.03(3)	S(7)–Si(8)–S(8)	107.54(3)
Si(1)–C(5)–Si(4)	121.71(11)	Si(5)–C(10)–Si(8)	121.62(11)

by 2.4 Hz (2%) in **7** and by 15 Hz (4%) in **8**. In general it can be stated that the ^{125}Te -NMR parameters (δ , $^1J_{\text{SiE}}$) parallel the ^{77}Se -NMR parameters with a factor of 2.5–2.6 [37].

Finally it should be mentioned that similar carbon based oxides, sulfides and selenides $(\text{MeC})_4(\text{CH}_2)_2\text{E}_4$ (E = O, S, Se) have been reported by Almqvist and Olsson [38–41]. The compounds were obtained by reaction of acetyl acetone with H_2E (E = O, S, Se) in glacial acetic acid in the presence of zinc chloride:



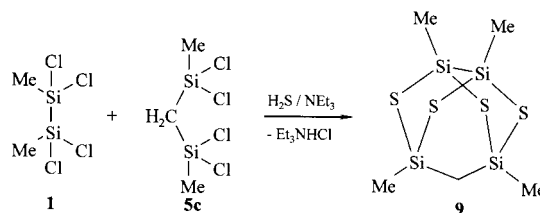
The carbon sesquichalcogenides $(\text{MeC})_4\text{E}_6$ (E = S, Se) were formed in a similar reaction of acetyl chloride:



A crystal structure analysis has been performed for $(\text{MeC})_4\text{S}_6$, showing angles at sulfur in the range of 102.7–103.5° [42], which is close to the SiSSi angles in $(\text{MeSi})_4\text{S}_6$ and **6**.

2.3. Silchalcogenanes $(\text{MeSi})_4(\text{CH}_2)_2\text{E}_4$ possessing noradamantane structures

Reaction of a 1:1 mixture of **1** and **5c** with H_2S and NEt_3 in hexane solution produced after workup the new noradamantane **9** besides small amounts of the adamantane compound **6**:

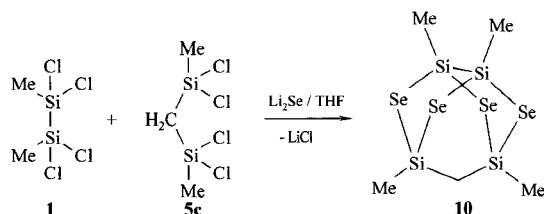


The molecular structure of **9** is shown in Fig. 5 revealing the noradamantane skeleton consisting of four silicon, four sulfur and one carbon atom. Some important bond parameters are summarized in Table 10. The very enlarged angles Si–C–Si at the methylene carbon atoms C(5) and C(10) of almost 122° are remarkable. The angles at the sulfur atoms are in the expected range for five-membered rings. In general the structure is very similar to that of **3**. Again, the four sulfur atoms form an almost ideal square with S–S distances of 3.46–3.52 Å and S–S–S angles between 89.5 and 90.3°. As in the noradamantane **3** the Si–Si bond is slightly longer than in other disilanes as a result of strain in the noradamantane cage.

Besides the NMR data, given in Table 9, **9** could also be identified by its mass spectrum.

If one compares the ^{29}Si -NMR shifts of **9** with those of the acyclic compounds $\text{Me}_2\text{Si}_2(\text{SBU})_4$ and $\text{Me}_2\text{Si}(\text{SBU})_2$ [21] the values are shifted to lower field by 14.0 ppm for the disilane unit and by 3.8 ppm for the two monosilane units. This is again in good agreement with the noradamantane structure where the disilane unit is part of five-membered rings which results always in a low field shift of this size as has already been discussed [19,23]. The monosilane units are part in both, five and six membered rings, which in its sum results in this case in a small low field shift.

The analogous selenium compound **10** could be produced by reacting a 1:1 mixture of **1** and **5c** with Li_2Se in THF whereas the reaction with Li_2Te did not yield any soluble products:



The assignment of the disilane unit of **10** in the ^{29}Si -NMR spectrum is simplified by the occurrence of $^1J_{\text{SiSe}}$ as well as $^2J_{\text{SiSe}}$ satellites besides the fact that the signal of the monosilyl units show two different $^1J_{\text{SiC}}$ satellites for the CH_3 and the CH_2 carbon atoms. Again, compared with the ^{29}Si chemical shifts of the acyclic compounds $\text{Me}_2\text{Si}(\text{SeBu})_2$ and $\text{Me}_2\text{Si}_2(\text{SeBu})_4$ [22] the disilane unit in **10** shows a strong low field shift of 24.1 ppm while the signal of the two monosilyl units remains almost unchanged (high field shift of 0.3 ppm) which is in accordance with the noradamantane structure.

3. Experimental

3.1. NMR and GC/MS measurements

All NMR spectra were recorded on a Bruker DPX 400 in CDCl_3 solution and TMS as internal standard for ^1H , ^{13}C and ^{29}Si . In order to get a sufficient signal/noise ratio of ^{29}Si -NMR spectra for obtaining $^1J_{\text{SiC}}$, $^1J_{\text{SiSi}}$, $^{1,2}J_{\text{SiSe}}$ or $^1J_{\text{SiTe}}$ satellites also ^{29}Si INEPT spectra were recorded. ^{77}Se and ^{125}Te spectra were recorded using an IGATED pulse program.

Mass spectra were measured on a Hewlett Packard 5971 (ionization energy: 70 eV, column: 30 m \times 0.25 mm \times 0.25 μm , phenylmethylpolysiloxane, column temperature: 80°C (3 min)/20 K min^{-1} , flow: He 0.5 ml min^{-1}).

3.2. Crystal structure analysis

X-ray structure analysis measurements were performed on a Bruker Smart CCD. Crystal data of **3**, **6**, **7**, **8**- CDCl_3 and **9** as well as data collection and refinement details are given in Table 11.

The unit cells were determined with the program SMART [43]. For data integration and refinement of the unit cells the program SAINT [43] was used. The space groups were determined using the program XPREP [43]. All data were corrected for absorption using SADABS [44]. The structures were solved using direct methods (SHELX-97 [45]), refined using least-squares methods (SHELX-97) and drawn using ZORTEP [46]. The ellipsoids at the nonhydrogen atoms are at the 50% probability level.

3.3. Starting materials

H_2S (N25, Air Liquide), Se, Te, triethylamine, 1 M $\text{Li}[\text{BEt}_3\text{H}]$ in THF (Super Hydride), and the used silanes MeSiCl_3 , $\text{MeCl}_2\text{Si}-\text{SiCl}_2\text{Me}$ and $\text{CH}_2(\text{SiMe}_3)_2$ were commercially available. THF was distilled from sodium potassium alloy prior to use. The other solvents were dried over KOH or sodium wire. All reactions were carried out under argon applying standard Schlenk techniques.

3.4. Noradamantanes $\text{Me}_4\text{Si}_4\text{E}_5$ ($\text{E} = \text{Se}$ (**3**), S (**4**)) and adamantanes $\text{Me}_4\text{Si}_4\text{E}_6$

A suspension of 0.2 g (2.5 mmol) powdered selenium in 5 ml THF was treated with 5 ml of a 1 M solution of $\text{Li}[\text{BEt}_3\text{H}]$ in THF under stirring. The solution became colorless and some white precipitation of Li_2Se occurred. 0.285 g (1.25 mmol) **1** were added under stirring at 0°C. The precipitation of Li_2Se disappeared and the solution became slightly yellow. After 20 min the solvent was removed in vacuo and replaced by 5 ml toluene. After stirring for 1 h the mixture was filtered from LiCl residue and yielded, after removal of the solvent, 0.18 g (50%) **4** as a white powder. Recrystallization from toluene gave very thin needles unsuitable for X-ray analysis. In air the crystals turn red (elemental selenium) within a short time.

The sulfur compound **3** was obtained by reacting a solution of 0.228 g (1 mmol) **1** and 0.299 g (2 mmol) MeSiCl_3 in 30 ml toluene with 1.4 ml (10 mmol) NET_3 while H_2S passed through the stirred solution for 30 min. A white precipitation of HNET_3Cl was formed, the mixture was filtered, and the solvent removed in vacuo. The resulting white crystals of **3** are well soluble in toluene and CDCl_3 but less in hexane. Single crystals were obtained from hexane solution.

3 GC/MS: m/e (rel. int.): 332 [M^+ , 75], 317 ($\text{M}-\text{Me}$, 2), 257 ($\text{Me}_3\text{Si}_3\text{S}_4$, 100), 227 ($\text{Me}_3\text{Si}_3\text{S}_4$, 3), 165

(Me₃Si₂S₂, 14), 135 (MeSi₂S₂, 9), 75 (MeSiS, 12), 73 (Me₃Si, 9).

The silsesquichalcogenides Me₄Si₄E₆ (E = S, Se) were prepared from MeSiCl₃ applying the procedures described above while the analogous reaction with Li₂Te (prepared in situ as described below) did not yield a toluene soluble product. The NMR data of the prepared silsesquichalcogenides were similar to reported values [7].

Me₄Si₄S₆ GC/MS: 364 [M⁺, 100], 349 (M–Me, 27), 257 (Me₃Si₃S₄, 68), 165 (Me₃Si₂S₂, 11), 135 (MeSi₂S₂, 6), 73 (Me₃Si, 6).

3.5. Chlorosubstituted disilylmethanes

CH₂(SiMe₃)₂ (4 g, 25 mmol) were mixed with 16 g (120 mmol) of anhydrous AlCl₃ and 9.5 g (120 mmol) acetyl chloride were slowly added under intensive stirring at room temperature. The mixture was heated under stirring for two hours (80–90°C) to give a homogeneous yellow oil. The product was extracted three times with 15 ml hexane and the combined hexane solutions were concentrated in vacuo to yield 4.3 g of a liquid residue containing 50% MeSiCl₂CH₂SiClMe₂ (**5b**) besides 45% MeSiCl₂CH₂SiCl₂Me (**5c**) and 5%

Table 11
Crystal data of **3**, **6**, **7**, **8**-CDCl₃ and **9** as well as data collection and refinement details

	3	6	7	8 -CDCl ₃	9
Crystal system	Monoclinic	Triclinic	Triclinic	Triclinic	Triclinic
Space group	<i>C</i> 2/ <i>c</i>	<i>P</i> $\bar{1}$	<i>P</i> $\bar{1}$	<i>P</i> $\bar{1}$	<i>P</i> $\bar{1}$
Unit cell dimensions					
<i>a</i> (Å)	16.2544(3)	9.5560(7)	9.1902(6)	9.0707(13)	9.4227(12)
<i>b</i> (Å)	21.2202(1)	9.9653(7)	9.5191(6)	10.8376(16)	10.2681(13)
<i>c</i> (Å)	13.9934(3)	10.2440(7)	10.0359(7)	12.5677(17)	15.2832(19)
α (°)	90	101.578(2)	93.4390(10)	72.891(3)	90.048(3)
β (°)	111.495(1)	108.065(2)	108.7810(10)	73.074(3)	91.896(3)
γ (°)	90	114.490(1)	99.9240(10)	87.304(3)	100.346(2)
<i>Z</i>	12	2	2	2	4
<i>V</i> (Å ³)	4490.93(13)	780.49(10)	812.48(9)	1128.6(3)	1453.8(3)
<i>D</i> _{calc} (g cm ⁻³)	1.477	1.399	2.111	2.443	1.438
Linear absorption coeff. (mm ⁻¹)	1.056	0.883	9.295	5.671	0.945
Radiation	Mo–K α	Mo–K α	Mo–K α	Mo–K α	Mo–K α
Temperature (K)	173(2)	173(2)	173(2)	173(2)	173(2)
Scan method	ω scans	ω scans	ω scans	ω scans	ω scans
Absorption correction	Empirical	Empirical	Empirical	Empirical	Empirical
Max./min. transmission	0.9017/0.8165	0.8738/0.6952	0.9467/0.5623	0.8049/0.0927	0.9282/0.5186
Measured reflections	10948	6529	6389	2224	11951
Independent reflections	5358	4259	4324	2224	7956
Observed reflections	3015	2840	2788	1768	5669
<i>R</i> _{int}	0.0659	0.0250	0.0325	0.0000	0.0220
θ Range for collection (°)	1.65–30.82	2.43–30.77	2.16–30.58	2.35–30.86	1.33–30.80
Completeness to θ_{\max} (%)	75.8	87.2	86.4	31.3	87.2
Refinement method	Full-matrix least-squares on <i>F</i> ²	Full-matrix least-squares on <i>F</i> ²	Full-matrix least-squares on <i>F</i> ²	Full-matrix least-squares on <i>F</i> ²	Full-matrix least-squares on <i>F</i> ²
Final <i>R</i> (<i>I</i> > 2 σ (<i>I</i>))	<i>R</i> ₁ : 0.0470	<i>R</i> ₁ : 0.0497	<i>R</i> ₁ : 0.0436	<i>R</i> ₁ : 0.0320	<i>R</i> ₁ : 0.0300
<i>R</i> (all data)	<i>R</i> ₁ : 0.1191	<i>R</i> ₁ : 0.0872	<i>R</i> ₁ : 0.0839	<i>R</i> ₁ : 0.0417	<i>R</i> ₁ : 0.0532
H-locating and refining	difmap/refall	difmap/refall	difmap/refall	difmap/refall	difmap/refall
Goodness-of-fit on <i>F</i> ²	0.927	1.018	0.955	1.101	0.959
Max./min. ρ density (e Å ⁻³)	0.394/–0.433	1.249/–0.781	0.982/–1.019	0.598/–0.721	0.372/–0.299

$\text{Me}_2\text{SiClCH}_2\text{SiClMe}_2$ (**5a**). To get pure **5c** the product was treated again with 2.7 g (20 mmol) AlCl_3 and 1.6 g (20 mmol) acetyl chloride for 4 h at 120°C . Work-up as described above yielded 2.5 g (10 mmol, 40%) pure **5c**, b.p.: 180°C .

Pure **5a** can be obtained if the molar ratio of $\text{CH}_2(\text{SiMe}_3)_2$: AlCl_3 : acetyl chloride is changed to 1:2:2 and the reaction is carried out at room temperature (yield: 40%).

5a: GC/MS: 185 (M–Me, 100), 165 (M–Cl, 15), 149 ($\text{ClMeSi}(\text{CH}_2)_2\text{SiMe}$, 10), 93 (Me_2SiCl , 18), 73 (Me_3Si , 9), 72 (Me_2SiCH_2 , 12), 63 (SiCl , 9)

5c: GC/MS: 227 (M–Me, 100), 205/207 (M–Cl, 9/9), 189/191 ($\text{Cl}_2\text{Si}(\text{CH}_2)_2\text{SiCl}$, 10/10), 113 (MeSiCl_2 , 19), 92 (MeSiClCH_2 , 27), 63 (SiCl , 25).

(The isotopic patterns are in all cases in agreement with the number of chlorine atoms of the fragments resulting in almost identical intensities of M and M + 2 peaks for three Cl atoms. In both mass spectra a fragment with a disilacyclobutane structure can be obtained).

3.6. Adamantanes $\text{Me}_4\text{Si}_4(\text{CH}_2)_2\text{E}_4$ (E = S (**6**), Se (**7**) and Te (**8**))

5c (0.36 g, 1.5 mmol) were dissolved in 20 ml toluene and 0.83 ml (6 mmol) NEt_3 were slowly added while H_2S bubbled through the solution. After filtration from precipitated HNEt_3Cl and removal of the solvent crystals of pure **6** were obtained which could be recrystallized from hexane, m.p.: 267°C .

6 GC/MS: 328 [M^+ , 100], 313 (M–Me, 93), 295 (10), 239 ($\text{Me}_3\text{Si}_3\text{S}_3\text{CH}_2$, 16), 221 ($\text{Me}_3\text{Si}_3\text{S}_2(\text{CH}_2)_2$, 19), 147 (6), 131 (Me_3Si_2 , 7), 75 (MeSiS , 4), 73 (Me_3Si , 5).

The selenium compound **7** was obtained by addition of 0.30 g (1.25 mmol) **5c** to a solution of 2.5 mmol Li_2Se in THF (freshly prepared from 0.2 g (2.5 mmol) Se, 5 ml THF and 5 ml of a 1 M solution of LiBEt_3H in THF). After work-up as described for the synthesis of **4** colorless needles of **7** were obtained, which could be recrystallized from toluene.

The tellurium compound **8** was prepared by essentially the same procedure as described for **7** but 0.32 g (2.5 mmol) tellurium powder were reacted with 5 ml of a 1 M solution of LiBEt_3H and 5 ml THF. But in contrast to Li_2Se , the formation of Li_2Te takes more than 1 h. The mixture turns initially deep purple and becomes light red finally. After addition of **5c** the solution turns yellow-brown. The colorless crystals of **8** are extremely sensitive towards moisture and air and turn black under formation of elemental tellurium.

3.7. Noradamantanes $\text{Me}_4\text{Si}_4(\text{CH}_2)\text{E}_4$ (E = S (**9**), Se (**10**))

Noradamantane **9** was prepared by reaction of a

mixture of 0.228 g (1 mmol) **1** and 0.242 g (1 mmol) **5c**, dissolved in 30 ml toluene, with H_2S and 1.1 ml (8 mmol) NEt_3 . After filtration and evaporation of the solvent a crystalline residue of **9** in mixture with some **6** was obtained. By fractional crystallization from hexane most of the much less soluble by-product **6** can be removed. The second fraction of crystals (0.15 g) consisted of 85% **9** besides 15% **6**, as determined by NMR.

9 GC/MS: 314 [M^+ , 93], 299 (M–Me, 12), 239 ($\text{Me}_3\text{Si}_3(\text{CH}_2)\text{S}_3$, 100), 147 (8), 131 (5), 75 (MeSiS , 7), 73 (Me_3Si , 4).

In analogy to the preparation of **7** a mixture of 0.228 g (1 mmol) **1** and 0.242 g (1 mmol) **5c** were added to 4 mmol freshly prepared Li_2Se in THF and after work-up as described for **4** a crystalline product mixture containing approximately 80% **10** besides 15% **7** and 5% **4** was isolated.

The analogous reaction with Li_2Te did not yield any soluble products.

4. Supplementary material

Crystallographic (excluding structure factors) data for the structural analysis have been deposited with the Cambridge Crystallographic Data Centre, CCDC nos. 154127–154131 for compounds **3**, **6**, **7**, **8**- CDCl_3 and **9**, respectively. Copies of this information may be obtained from The Director, CCDC, 12 Union Road, Cambridge CB2 1EZ, UK (fax: +44-1233-336-033; e-mail: deposit@ccdc.cam.ac.uk or www: <http://www.ccdc.cam.ac.uk>).

Acknowledgements

The authors wish to thank the ‘Deutsche Forschungsgemeinschaft’ for financial support. Special thanks are given to Professor H. Lang, Chair of Inorganic Chemistry, TU Chemnitz for the access to the X-ray facility used to determine the single crystal structures.

References

- [1] M.G. Voronkov, V.I. Lavrent'yev, Top. Curr. Chem. 102 (1982) 199.
- [2] R. Baney, M. Itoh, A. Sakakibara, T. Suzuki, Chem. Rev. 95 (1995) 1409.
- [3] F.J. Feher, T.A. Budzichowski, Polyhedron 14 (1995) 3239.
- [4] J.D. Lichtenhan, in: J.C. Salamone (Ed.), Polymeric Material Encyclopedia, vol. 10, CRC Press, New York, 1996, pp. 7768–7778.
- [5] J.C.J. Bart, J.J. Daly, J. Chem. Soc. Dalton Trans. (1975) 2063.
- [6] A. Haas, R. Hitze, C. Krüger, K. Angermund, Z. Naturforsch. Teil. B 39 (1984) 890.
- [7] S.R. Bahr, P. Boudjouk, Inorg. Chem. 31 (1992) 712.

- [8] R.H. Benno, C.J. Fritchie, *J. Chem. Soc. Dalton Trans.* (1973) 543.
- [9] A. Müller, R. Christophliemk, H.P. Ritter, *Z. Naturforsch. Teil B* 28 (1973) 519.
- [10] A. Haas, H.-J. Kutsch, C. Krüger, *Chem. Ber.* 120 (1987) 1045.
- [11] C. Dörfelt, A. Janeck, D. Kobelt, E.F. Paulus, H. Scherer, *J. Organomet. Chem.* 14 (1968) P22.
- [12] D. Kobelt, E.F. Paulus, H. Scherer, *Acta Crystallogr. Sect. B* 28 (1972) 2323.
- [13] H. Berwe, A. Haas, *Chem. Ber.* 120 (1987) 1175.
- [14] A. Blecher, M. Dräger, B. Mathiasch, *Z. Naturforsch. Teil B* 36 (1981) 1361.
- [15] M. Unno, Y. Kawai, H. Shioyama, H. Matsumoto, *Organometallics* 16 (1997) 4428.
- [16] W. Ando, T. Kadowaki, Y. Kabe, M. Ishii, *Angew. Chem. Int. Ed. Engl.* 31 (1992) 59.
- [17] K. Merzweiler, U. Lindner, in: N. Auner, J. Weis (Eds.), *Organosilicon Chemistry II*, VCH, Weinheim, 1996, pp. 531–539.
- [18] W. Ando, T. Kadowaki, A. Watanabe, N. Choi, Y. Kabe, T. Erata, M. Ishii, *Nippon Kagaku Kaishi* (1994) 214.
- [19] U. Herzog, U. Böhme, G. Roewer, G. Rheinwald, H. Lang, *J. Organomet. Chem.* 602 (2000) 193.
- [20] E. Lukevics, O. Pudova, *Main Group Metal Chem.* 21 (1998) 123.
- [21] U. Herzog, G. Roewer, *Main Group Metal Chem.* 22 (1999) 579.
- [22] U. Herzog, *J. Prakt. Chem.* 342 (2000) 379.
- [23] U. Herzog, U. Böhme, G. Rheinwald, *J. Organomet. Chem.* 612 (2000) 133.
- [24] H. Sakurai, K. Tominaga, T. Watanabe, M. Kumada, *Tetrahedron Lett.* 45 (1966) 5493.
- [25] G. Déléris, M. Birot, J. Dunoguès, *J. Organomet. Chem.* 266 (1984) 1.
- [26] B. Gehrhus, P.B. Hitchcock, M.F. Lappert, J. Heinicke, R. Boese, D. Bläser, *J. Organomet. Chem.* 521 (1996) 211.
- [27] M. Weisenbruch, L. Kirmaier, E. Kroke, W. Saak, *Z. Anorg. Allg. Chem.* 623 (1997) 1227.
- [28] B.O. Dabbousi, P.J. Bonasia, J. Arnold, *J. Am. Chem. Soc.* 113 (1991) 3186.
- [29] P.J. Bonasia, D.E. Gindelberger, B.O. Dabbousi, J. Arnold, *J. Am. Chem. Soc.* 114 (1992) 5209.
- [30] D.E. Gindelberger, J. Arnold, *J. Am. Chem. Soc.* 114 (1992) 6242.
- [31] P.J. Bonasia, J. Arnold, *Inorg. Chem.* 31 (1992) 2508.
- [32] P.J. Bonasia, V. Christou, J. Arnold, *J. Am. Chem. Soc.* 115 (1993) 6777.
- [33] D.E. Gindelberger, J. Arnold, *Organometallics* 13 (1994) 4462.
- [34] R.P.-K. Tan, G.R. Gillette, D.R. Powell, R. West, *Organometallics* 10 (1991) 546.
- [35] P. Jutzi, A. Möhrke, A. Müller, H. Bögge, *Angew. Chem. Int. Ed. Engl.* 28 (1989) 1518.
- [36] U. Herzog, *Main Group Metal Chem.* 24 (2001) 31.
- [37] U. Herzog, G. Rheinwald, *J. Organomet. Chem.* 627 (2001) 144.
- [38] S.-O. Almqvist, *Acta Chem. Scand.* 22 (1968) 1367.
- [39] K. Olsson, *Acta Univ. Upsaliensis, Abstr. Uppsala Dissertations Sci.* 102 (1967).
- [40] K. Olsson, S.-O. Almqvist, *Arkiv Kemi* 27 (1967) 571.
- [41] K. Olsson, S.-O. Almqvist, *Acta Chem. Scand.* 23 (1969) 3271.
- [42] J. Pickardt, N. Rautenberg, *Z. Naturforsch. Teil B* 41 (1986) 409.
- [43] Bruker AXS Inc., Madison, WI, 1998.
- [44] SADABS: area-detector absorption correction, Siemens Industrial Automation Inc., Madison, WI, 1996.
- [45] G.M. Sheldrick, *SHELX-97* (includes *SHELXS-97*, *SHELXL-97*, *CIFTAB*), programs for crystal structure analysis (release 97-2), University of Göttingen, Germany, 1997.
- [46] L. Zsolnai, G. Huttner, *ZORTEP*, University of Heidelberg, Germany, 1994.